

Observed Point-Specific Surface Temperatures Are Poor Indicators Of Global Temperature Change And Surface Radiative Forcing

**Roger A. Pielke Sr.
Colorado State University
and Duke University**

**Presented at the NRC Committee Meeting on Radiative
Forcing Effects on Climate, Washington, DC**

December 18, 2003

The following slides are from Davey, C.A., and R.A. Pielke Sr., 2003: Microclimate exposures of surface-based weather stations - implications for the assessment of long-term temperature trends. *Bull. Amer. Meteor. Soc.*, submitted

<http://blue.atmos.colostate.edu/publications/pdf/R274.pdf>

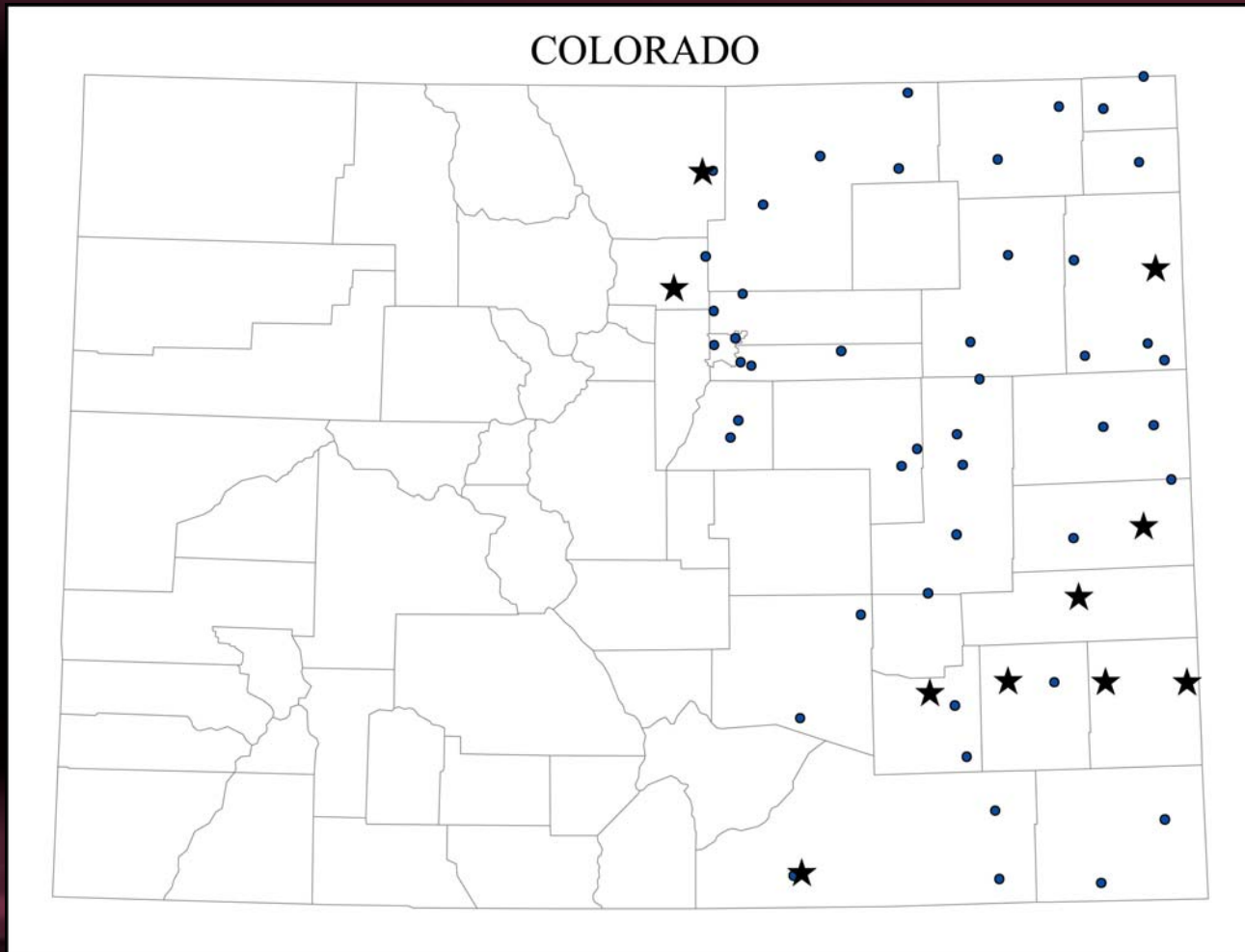
Maximum-minimum temperature sensor (MMTS) installation near Lindon, Colorado.



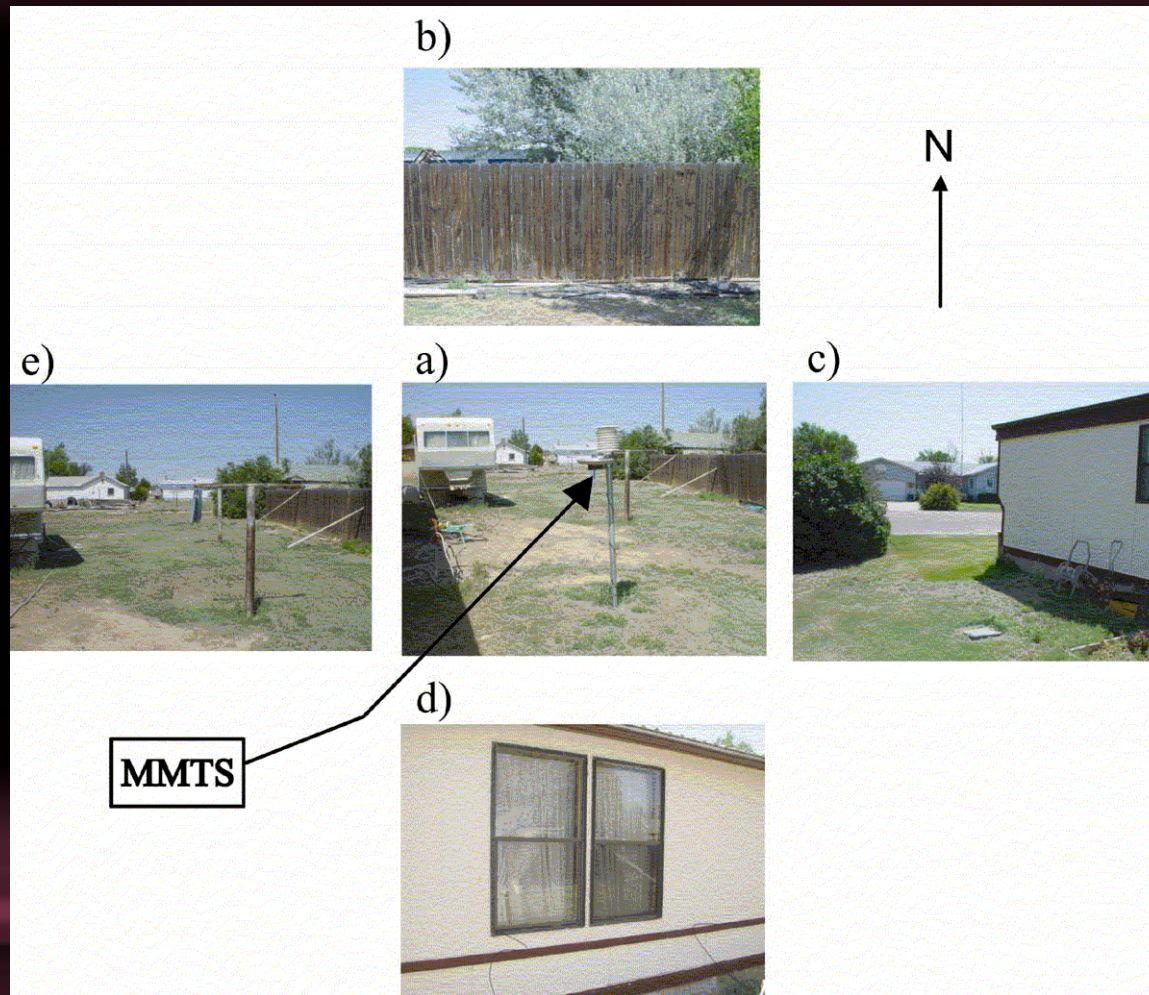
MMTS installation near John Martin Reservoir, Colorado.



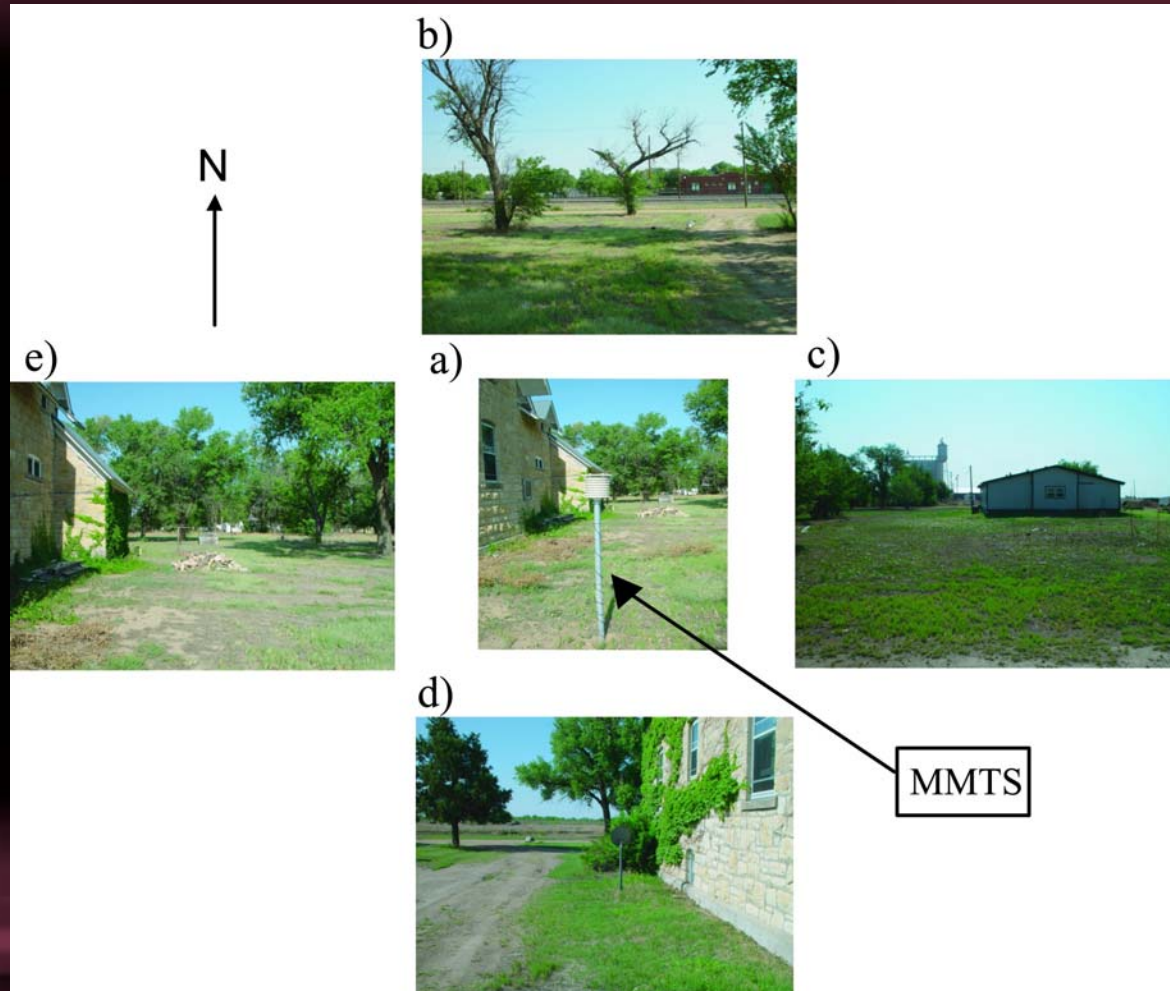
Map of study region, showing all surveyed COOP sites. The USHCN sites are indicated by stars.



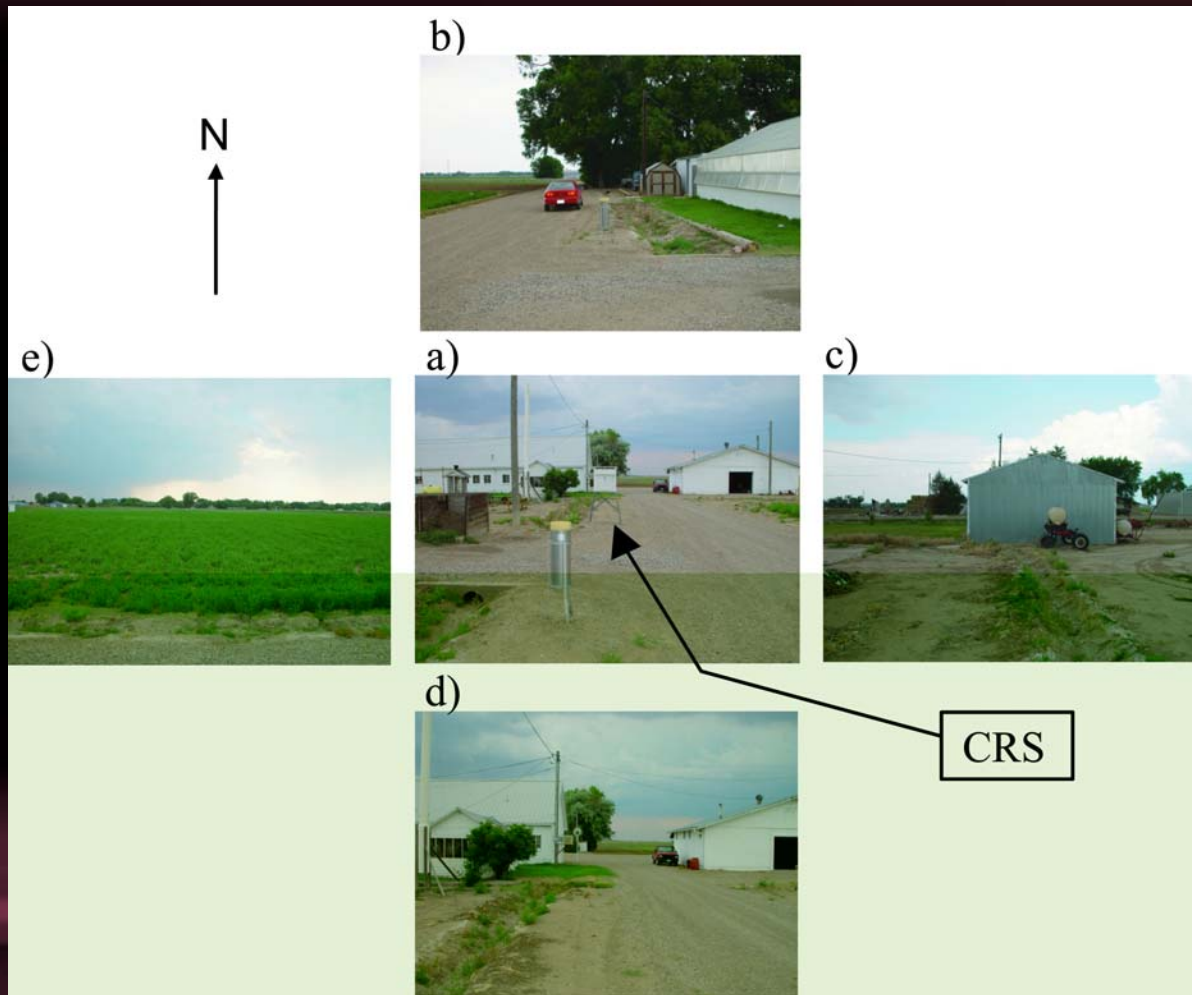
Photographs of the temperature sensor exposure characteristics of the NWS COOP station at Eads, CO. Panel a) shows the temperature sensor, while panels b)-e) illustrate the exposures viewed from the temperature sensor looking N, E, S, and W, respectively.



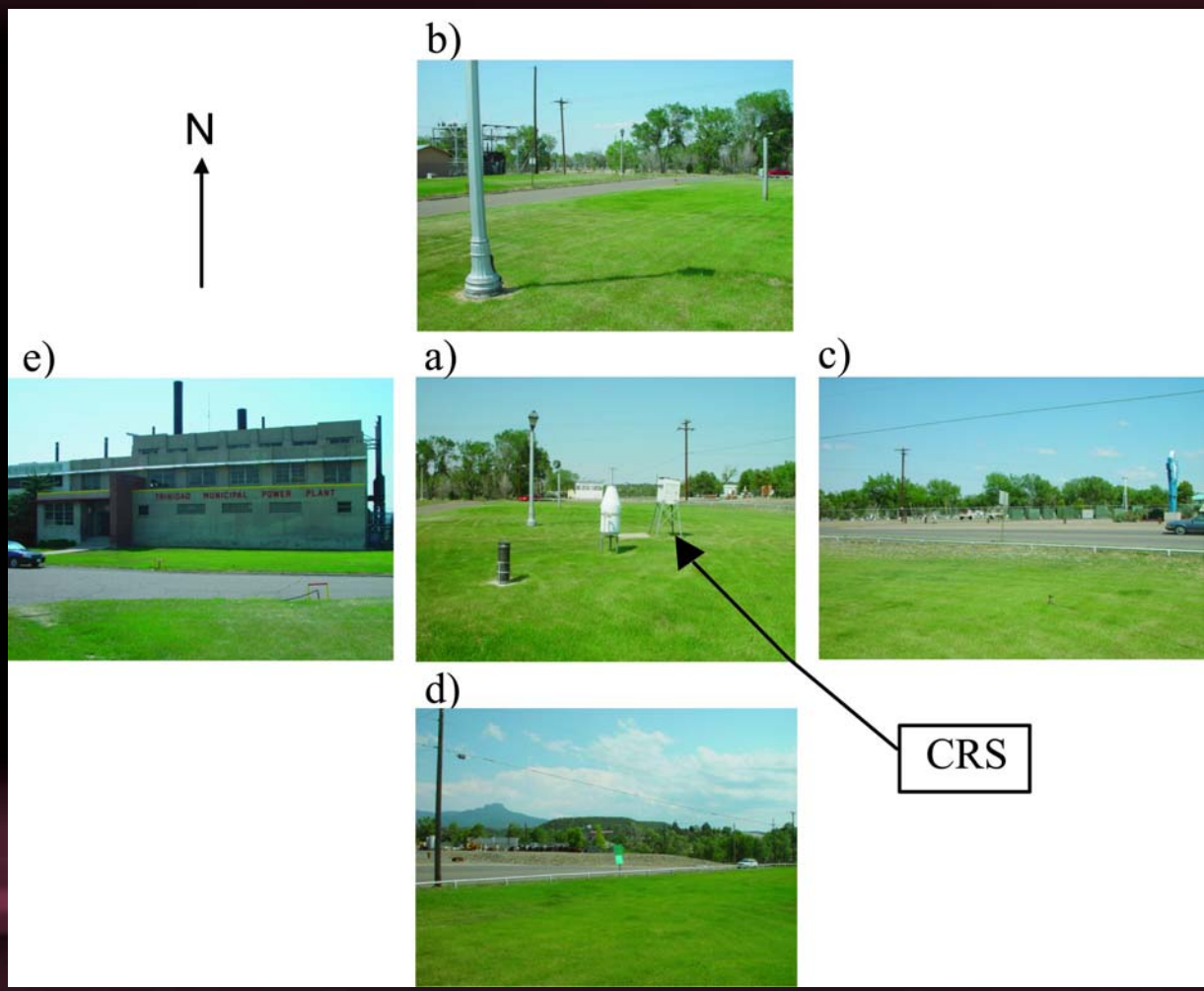
Photographs of the temperature sensor exposure characteristics of the NWS COOP station at Holly, CO. Panel a) shows the temperature sensor, while panels b)-e) illustrate the exposures viewed from the temperature sensor looking N, E, S, and W, respectively.



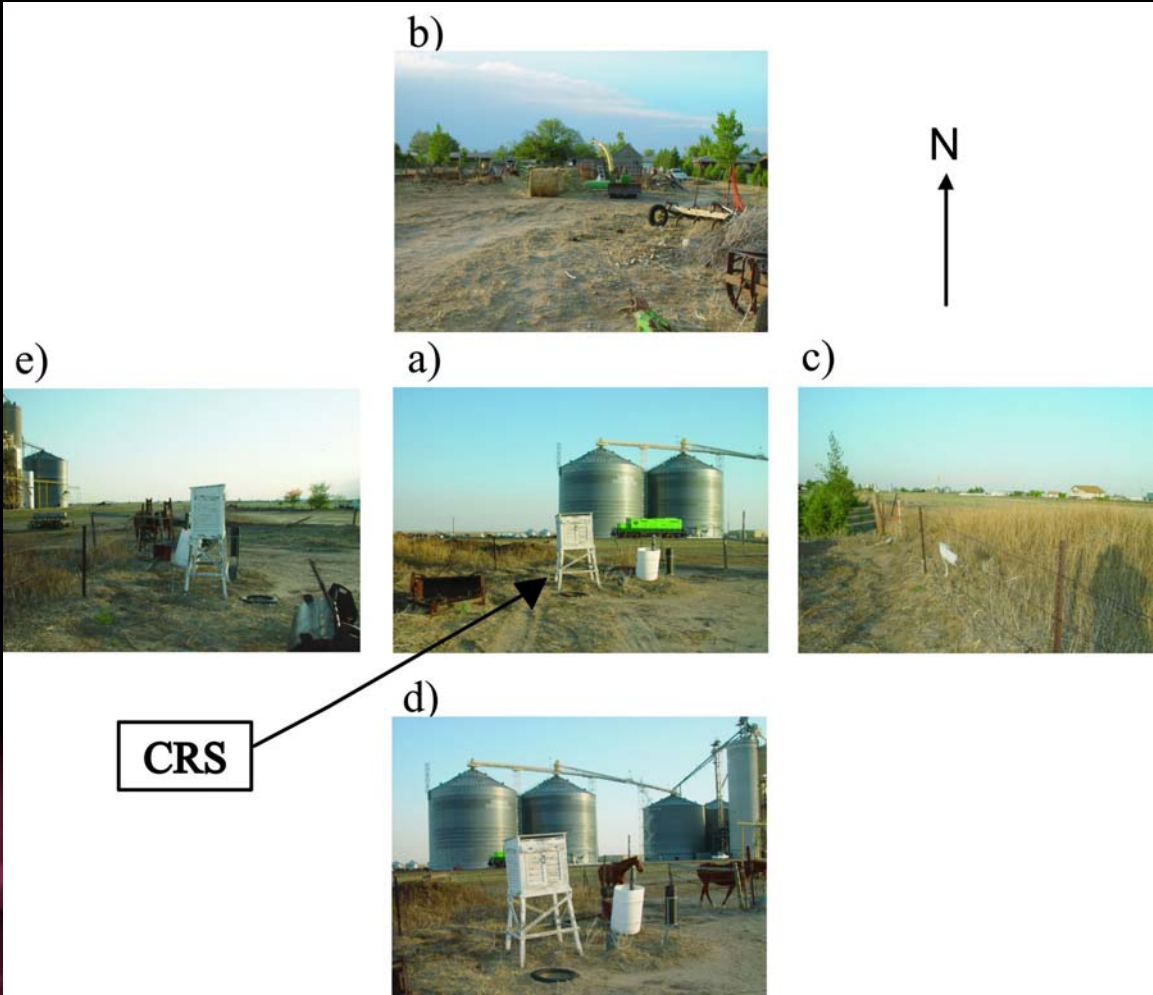
Photographs of the temperature sensor exposure characteristics for the NWS COOP station near Rocky Ford, Colorado. Panel a) shows the temperature sensor, while panels b)-e) illustrate the exposures viewed from the temperature sensor looking N, E, S, and W, respectively. (CRS-Cotton Region Shelter)



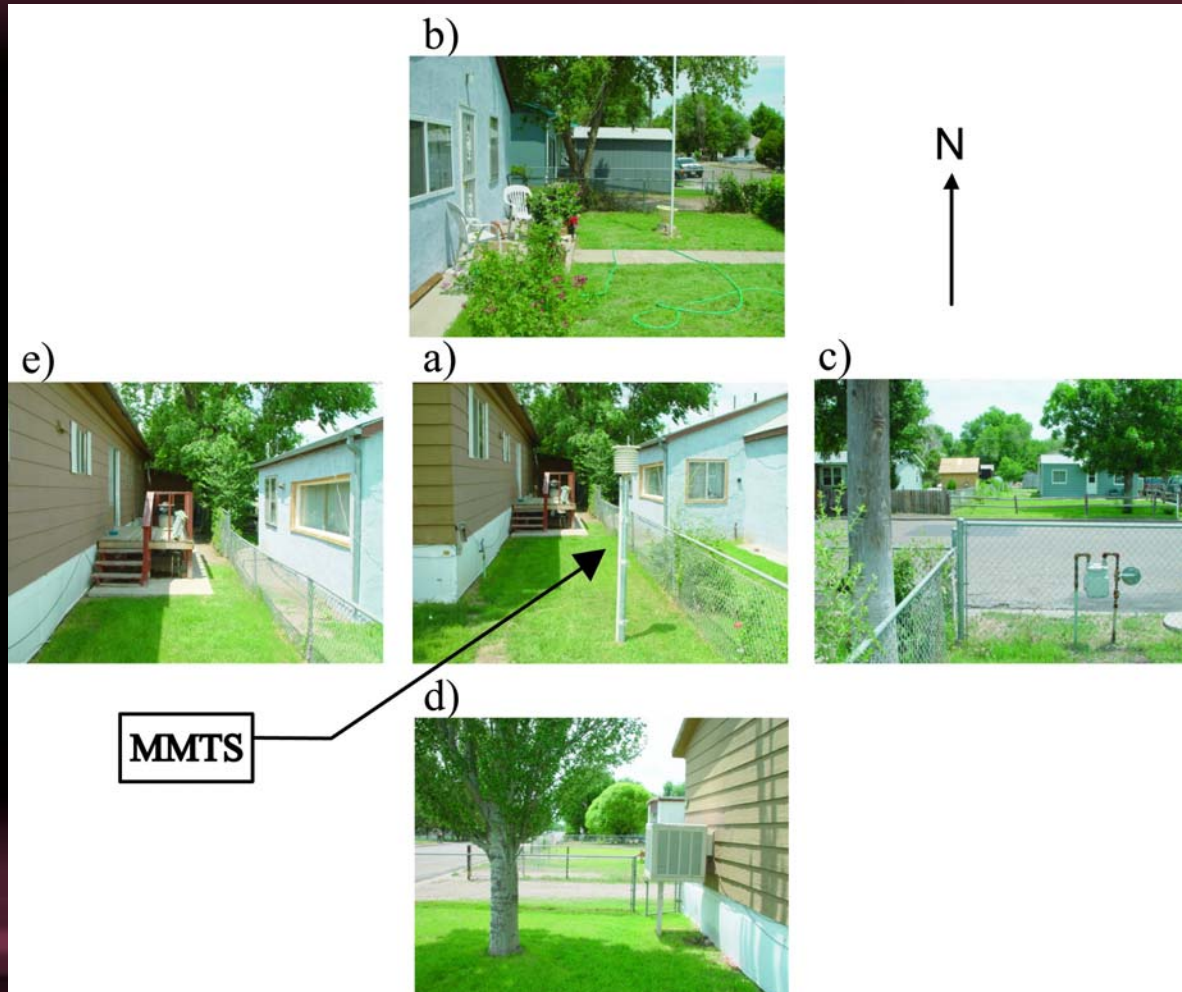
Photographs of the temperature sensor exposure characteristics of the NWS COOP station at Trinidad, Colorado. Panel a) shows the temperature sensor, while panels b)-e) illustrate the exposures viewed from the temperature sensor looking N, E, S, and W, respectively.



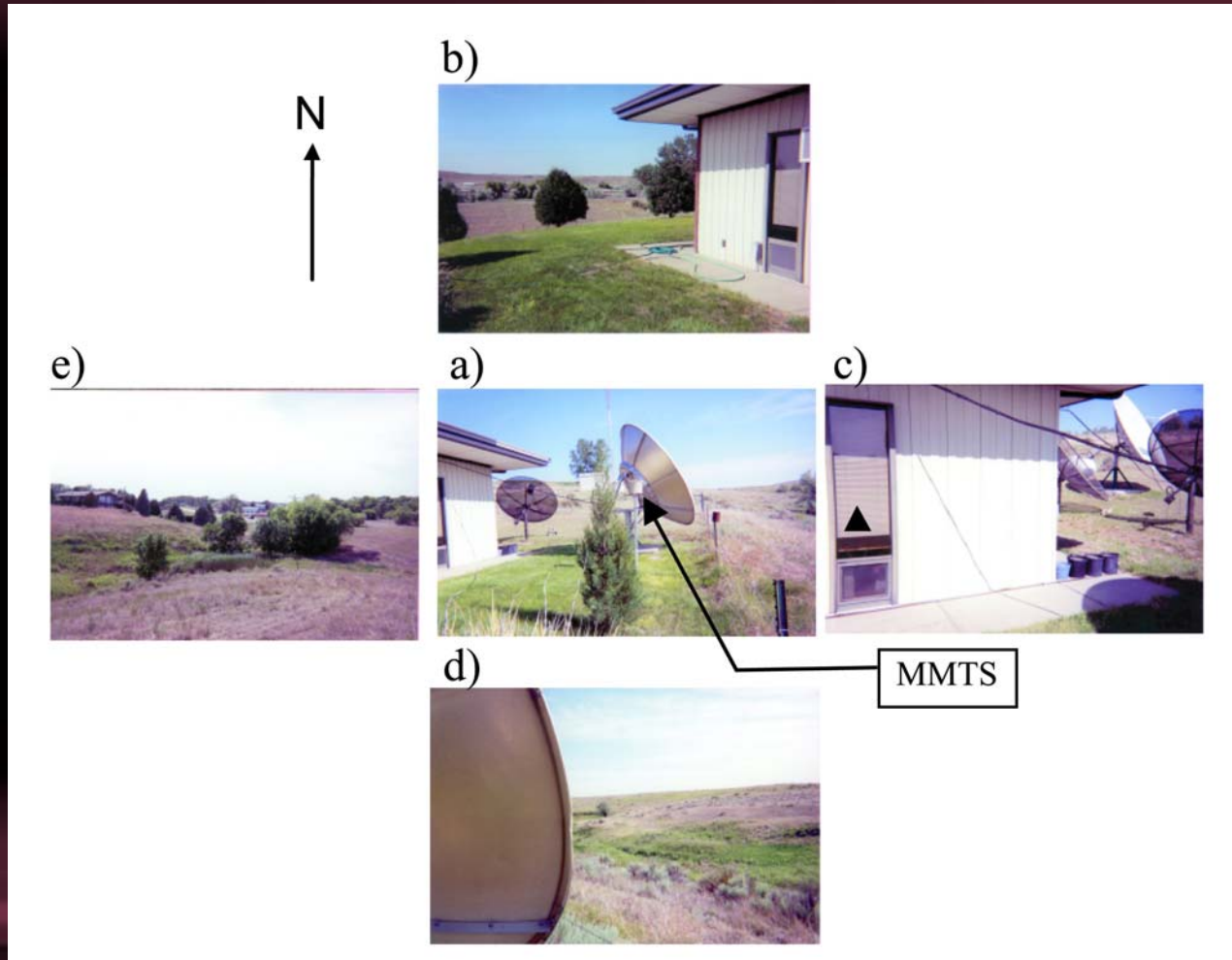
Photographs of the temperature sensor exposure characteristics of the NWS COOP station at Cheyenne Wells, Colorado. Panel a) shows the temperature sensor, while panels b)-e) illustrate the exposures viewed from the temperature sensor looking N, E, S, and W, respectively.



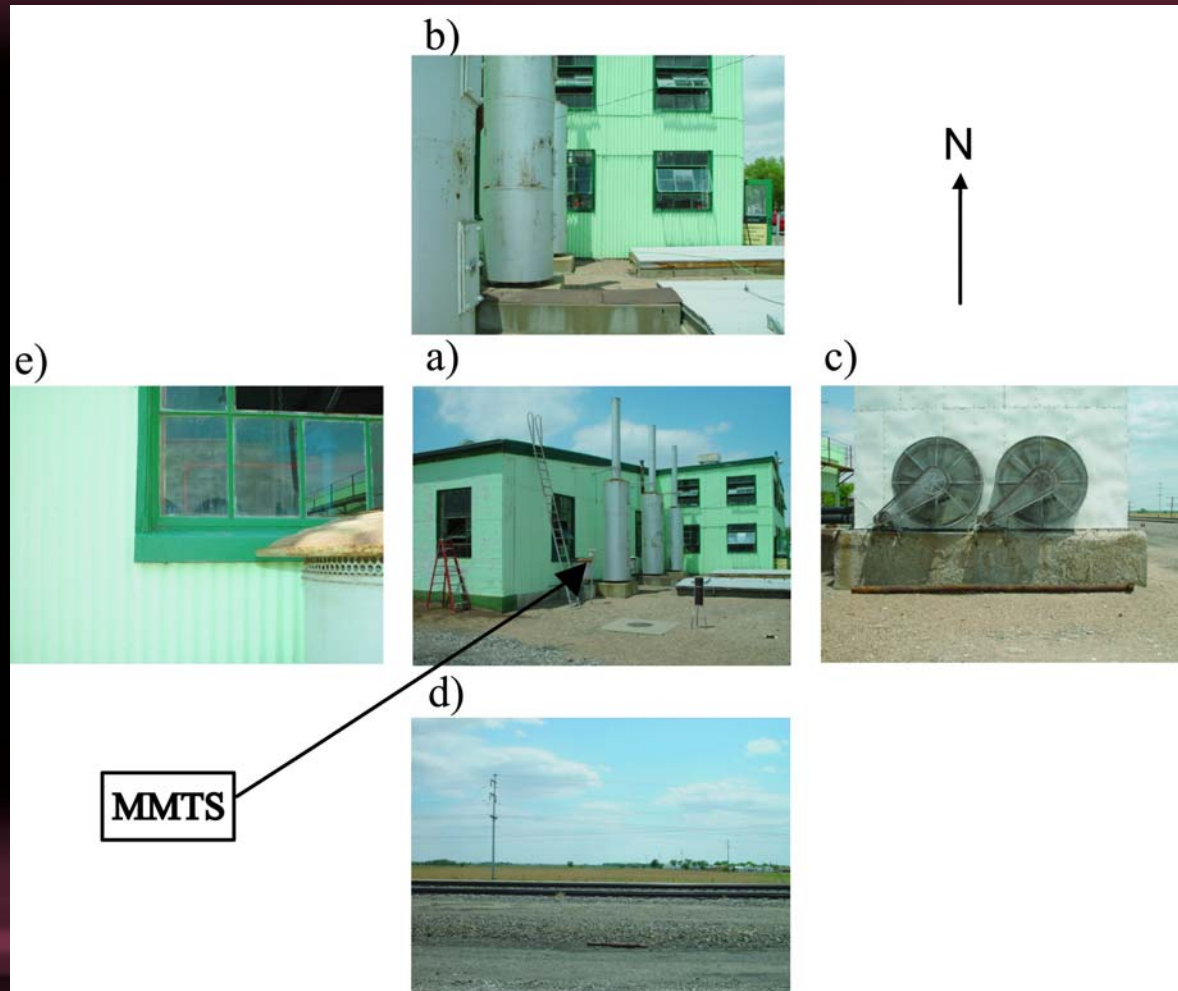
Photographs of the temperature sensor exposure characteristics of the NWS COOP station at Lamar, Colorado. Panel a) shows the temperature sensor, while panels b)-e) illustrate the exposures viewed from the temperature sensor looking N, E, S, and W, respectively.



Photographs of the temperature sensor exposure characteristics of the NWS COOP station at Wray, Colorado. Panel a) shows the temperature sensor, while panels b)-e) illustrate the exposures viewed from the temperature sensor looking N, E, S, and W, respectively.



Photographs of the temperature sensor exposure characteristics of the NWS COOP station at Las Animas, Colorado. Panel a) shows the temperature sensor, while panels b)-e) illustrate the exposures viewed from the temperature sensor looking N, E, S, and W, respectively.



**Ocean Heat Content Provides
An Effective Metric Of
The Global Radiative
Forcing Imbalance**

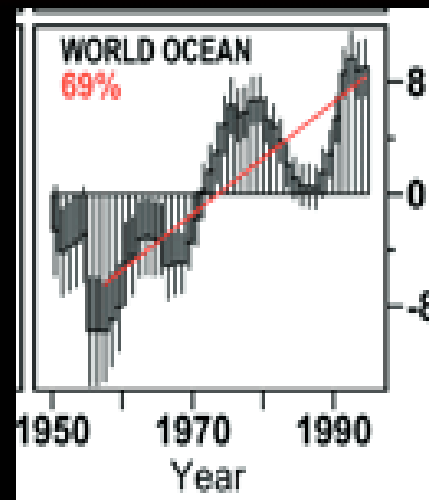
The heat budget for the earth system can be expressed as

$$\iint_{t, A_{\text{Earth}}} R_N dA dt = \iint_{t, V_{\text{atmos}}} Q dV dt + \iint_{t, V_{\text{ocean}}} Q dV dt \quad (1)$$

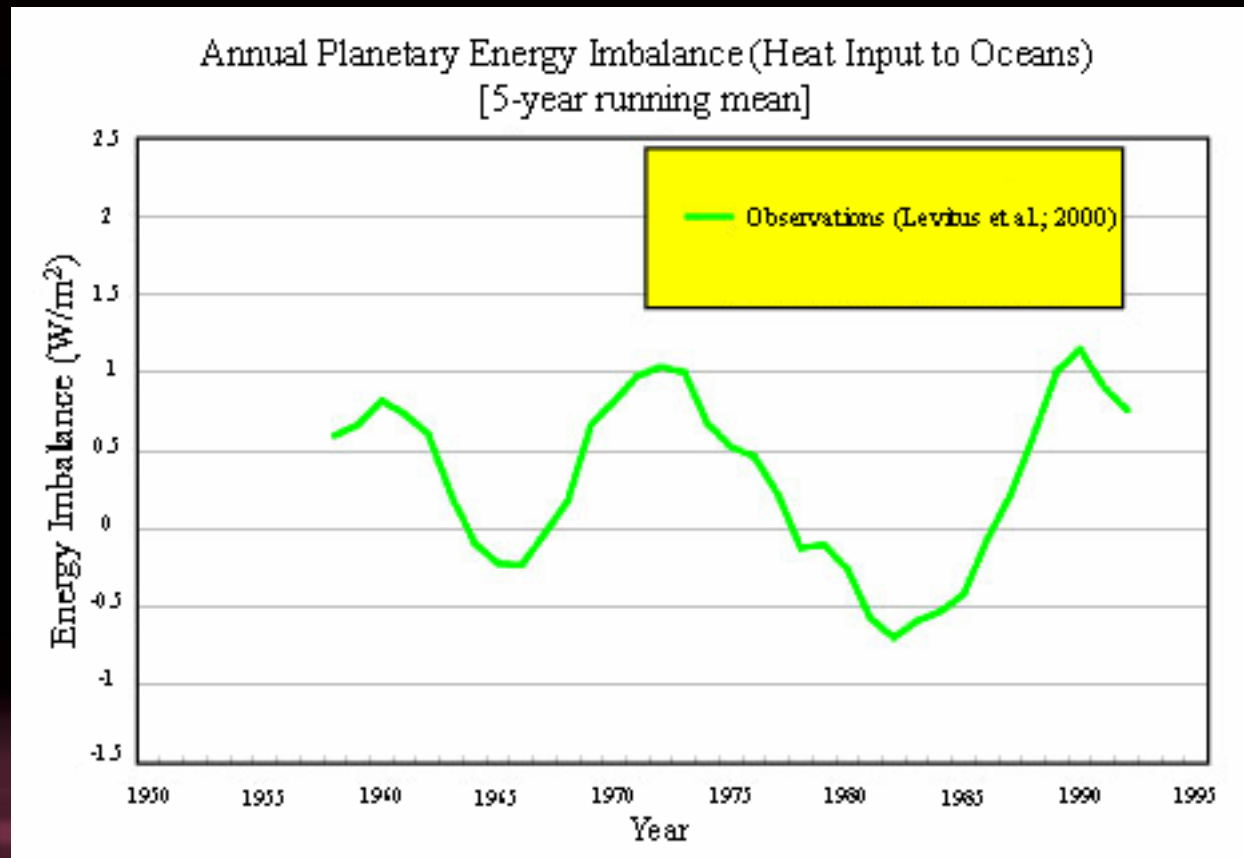
+ other heat reservoirs,

where R_N is the global mean nonequilibrium radiative forcing, A_{Earth} is the area of the earth, Q is the heating rate, V_{atmos} is the volume of the atmosphere, and V_{ocean} is the volume of the ocean.

Time series of 5-year running composites of heat content (10^{22} J) in the upper 3000 m for the world ocean. Vertical lines represent ± 1 SE of the 5-year mean estimate of heat content. The linear trend is estimated for each time series for the period 1955 to 1996, which corresponds to the period of best data coverage. The trend is plotted as a red line. The percent variance accounted for by this trend is given in the upper left corner. From Levitus et al. 2000: Warming of the World Ocean, Science, March 24; 287: 2225-2229.



Planetary energy imbalance (heat storage in the upper 3 km of the world ocean) observations expressed in units of watts m⁻² (adapted from Levitus et al. 2001). (Figure prepared by Alan Robock, Rutgers University, 2001, personal communication.)

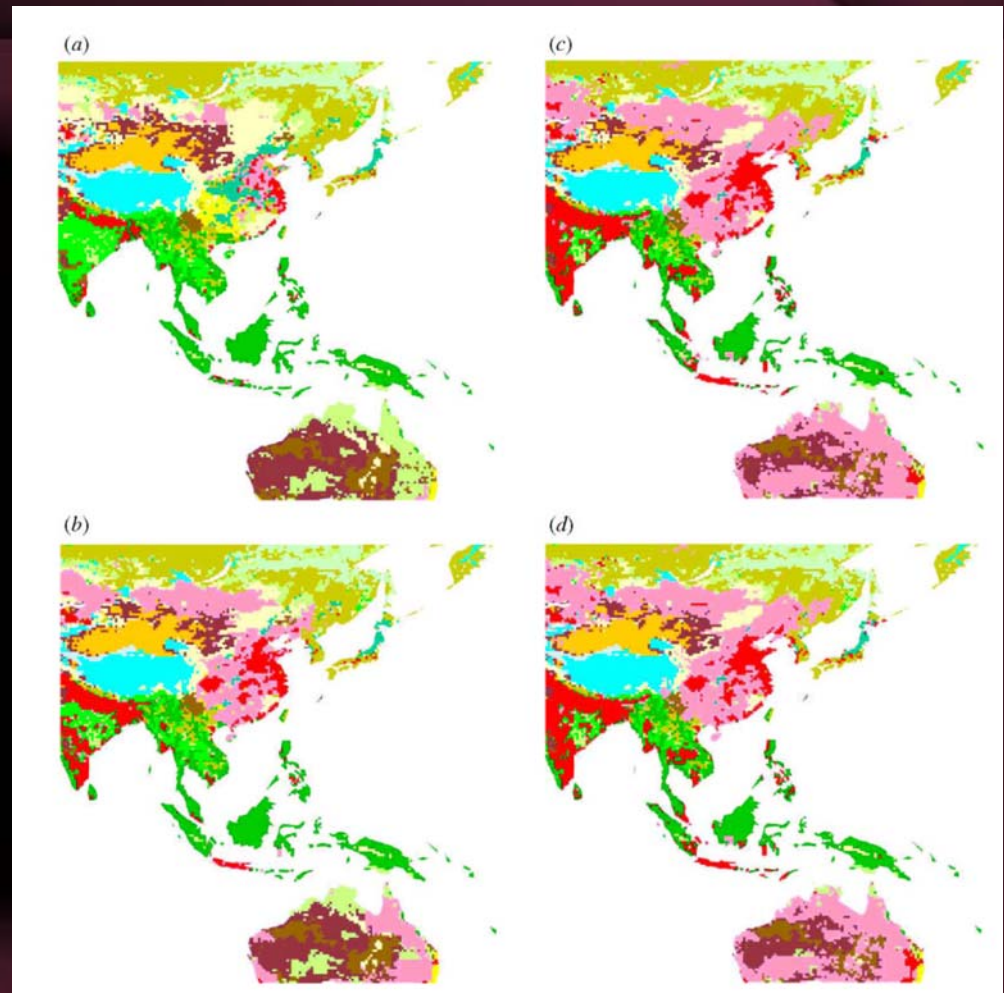


The Spatial Structure Of Radiative Heating Has A Major Effect On Global Climate

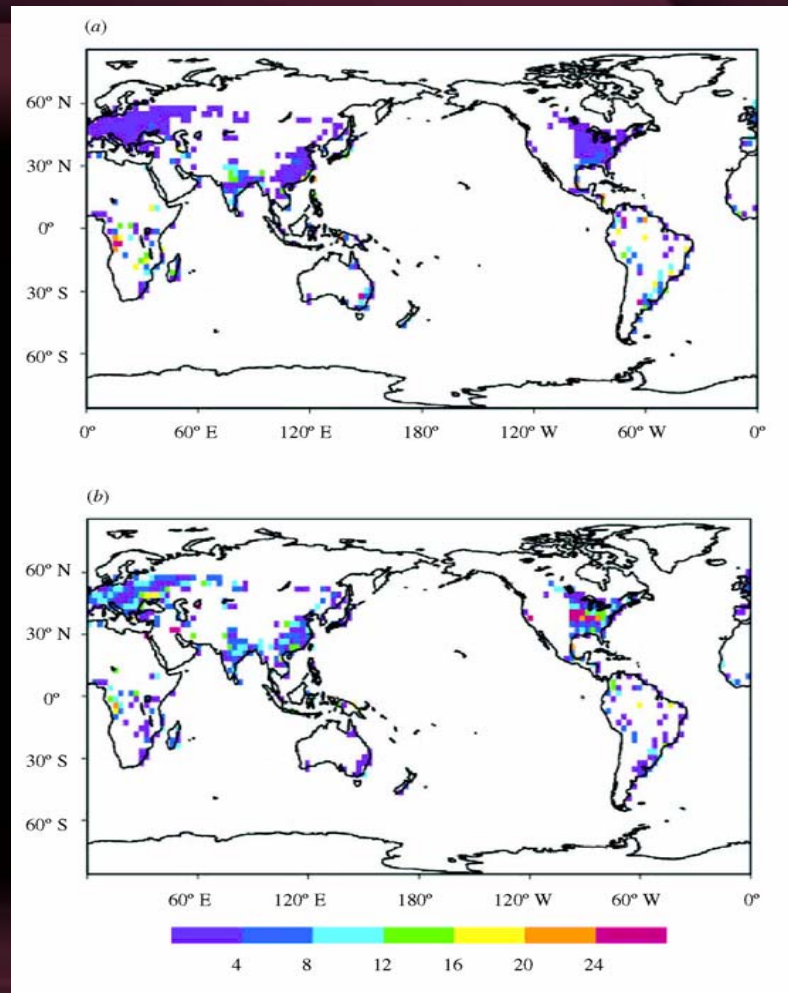
From Pielke Sr., R.A., G. Marland, R.A. Betts, T.N. Chase, J.L. Eastman, J.O. Niles, D. Niyogi, and S. Running, 2002: The influence of land-use change and landscape dynamics on the climate system- relevance to climate change policy beyond the radiative effect of greenhouse gases. *Phil. Trans. A. Special Theme Issue*, 360, 1705-1719.

R-258 at <http://blue.atmos.colostate.edu/publications/reviewedpublications.shtml>

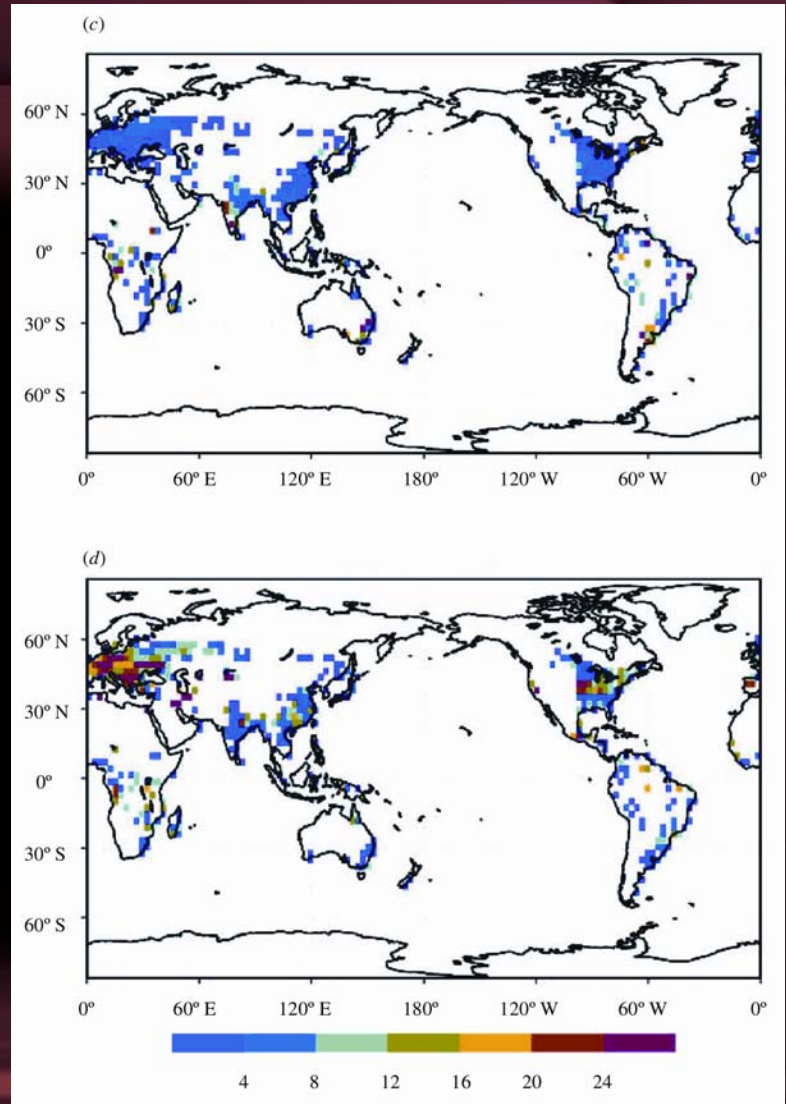
Examples of land-use change from (a) 1700, (b) 1900, (c) 1970, and (d) 1990. The human-disturbed landscape includes intensive cropland (red) and marginal cropland used for grazing (pink). Other landscape includes tropical evergreen forest and deciduous forest (dark green), savannah (light green), grassland and steppe (yellow), open shrubland (maroon), temperate deciduous forest (blue), temperate needleleaf evergreen forest (light yellow) and hot desert (orange). Note the expansion of cropland and grazed land between 1700 and 1900. (Reproduced with permission from Klein Goldewijk 2001.)



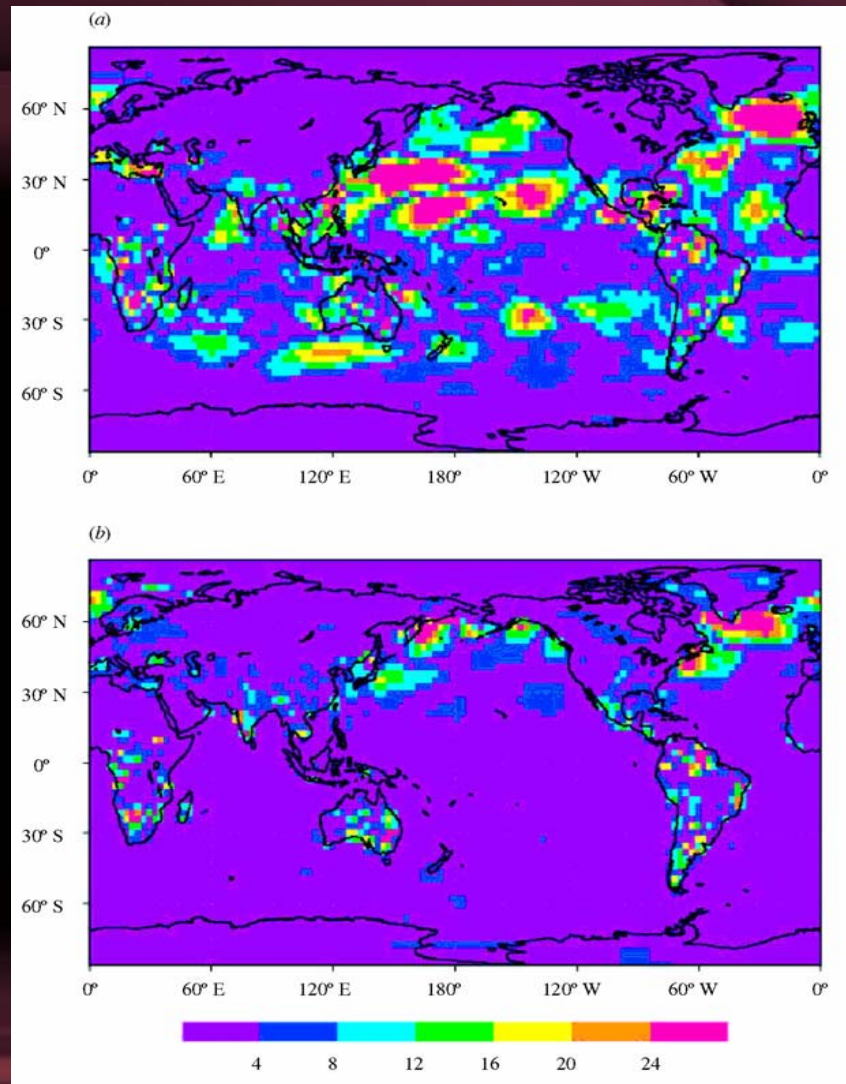
The ten-year average absolute-value change in surface latent turbulent heat flux in $W m^{-2}$ at the locations where land-use change occurred for (a) January, and (b) July. (Adapted from Chase et al. 2000.)



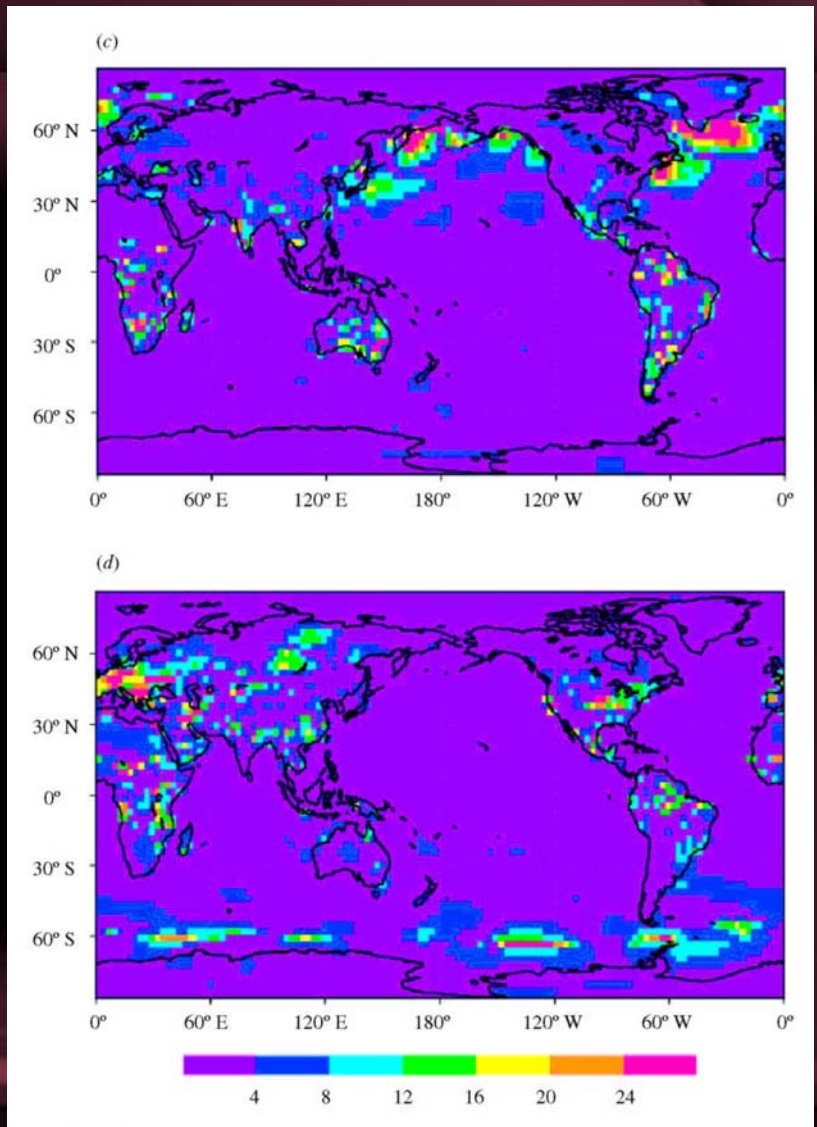
The ten-year average absolute-value change in surface sensible heat flux in $W m^{-2}$ at the locations where land-use change occurred for (c) January, and (d) July. (Adapted from Chase et al. 2000.)



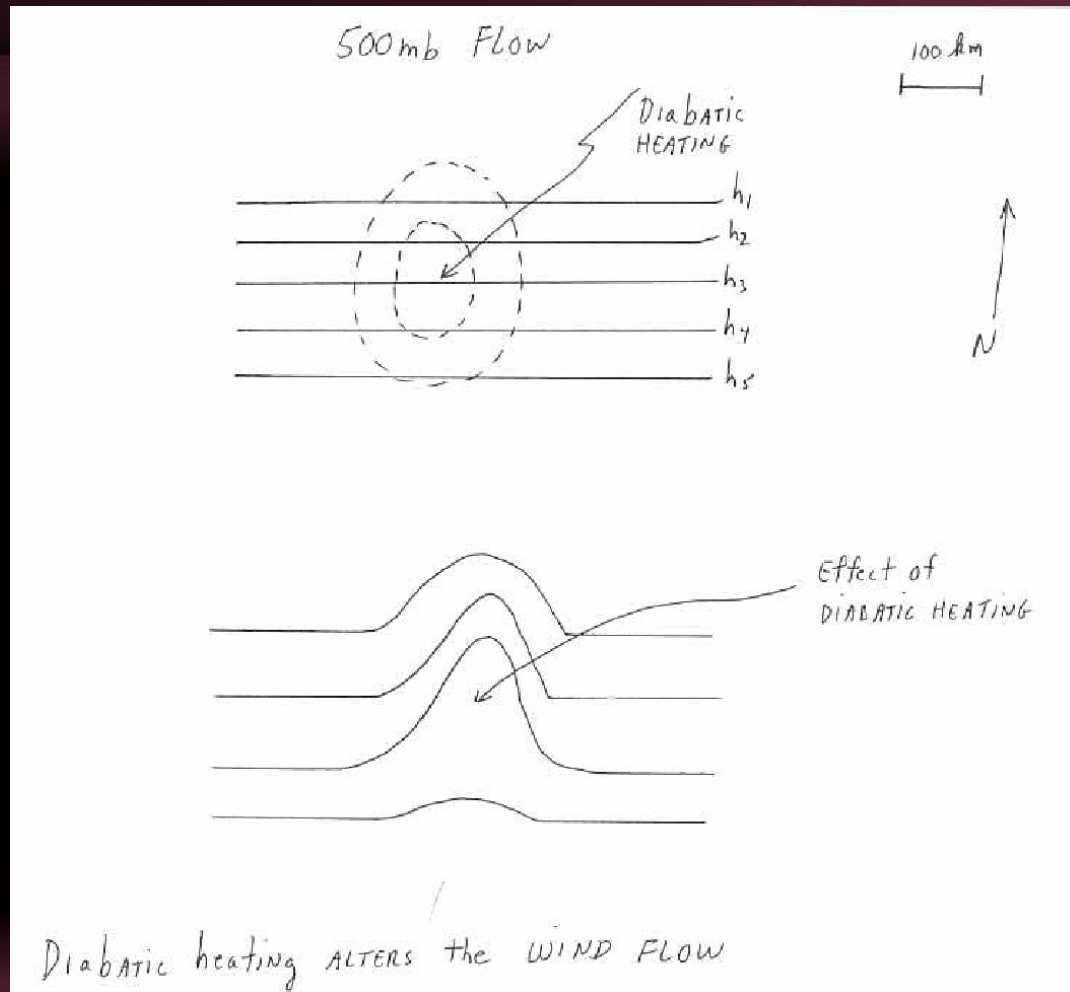
The ten-year average absolute-value change in surface latent turbulent heat flux in $W m^{-2}$ worldwide as a result of the land-use changes for (a) January, and (b) July. (Adapted from Chase et al. 2000.)



The ten-year average absolute-value change in sensible turbulent heat flux in $W m^{-2}$ worldwide as a result of the land-use changes for (c) January, and (d) July. (Adapted from Chase et al. 2000.)



Effect of Spatial Anomalies of Heating



Magnitude of Effect

A value of heat flux of 50 W m^{-2} correspond to a heating rate of about 0.8C d^{-1} if distributed throughout the 1000 to 500 mb layer. In terms of a thickness gradient change, this corresponds to about 20 m d^{-1} . Using a 500 km distance for the spatial gradient, the wind speed at 500 mb would increase by $4 \text{ m s}^{-1} \text{ d}^{-1}$. The cumulative effect of this gradient would be of the order of $28 \text{ m s}^{-1} \text{ week}^{-1}$.

From Pielke, R.A. and P.L. Vidale, 1995: The boreal forest and the polar front. J. Geophys. Res., 100, 25755-25758

Available at <http://blue.atmos.colostate.edu/publications/pdf/R-200.pdf>